Nanoscale Precipitation Strengthening of the Al(Sc,Ti) Alloys

Undergraduate Researcher
Arkadiusz Stachurski, Dominican University, Chicago, Illinois

Faculty Mentor
David Seidman
Department of Materials Science and Engineering, Northwestern University

Graduate Student Mentors
Marsha Van Dalen and Richard Karnesky
Department of Materials Science and Engineering, Northwestern University

Abstract

This study investigated the precipitation strengthening of the binary Al-0.14wt% Sc, 0.16% Ti alloy system. Ingots of Al-2.1wt% Sc and Al-4.68wt% Ti were melted together, and the nucleation, growth, and coarsening of precipitates were analyzed. The microstructural evolution of the nanoscale L12 precipitates phase was examined with Vickers microhardness testing, transmission electron microscopy (TEM), and three-dimensional atom probe (3DAP). The chemical identities of the individual atoms, as well as the mechanical properties of the ternary alloy annealed at 300˚C for hours, were thus measured. Careful examination of the 3DAP data and the concentration profiles of the analyzed Al(Sc,Ti) alloy proved that the Ti partitioned and/or substituted into the $Al_3(Sc)$ precipitate. This Ti propagation decreased the lattice mismatch between the Al matrix and the $Al_3(Sc_{1-x}Ti_x)$ precipitates. This study attempted to determine if the partitioning of the Ti in the system would decrease the coarsening rate and increase the creep resistance properties of the alloy. Further analysis of the alloy at higher temperatures and longer aging times is required, however, since the microhardness values of the Al-0.14wt% Sc, 0.16% Ti were not considerably augmented in comparison with the Al-0.1wt% Sc binary two-phase alloy system previously studied.

Introduction

Aluminum (Al) is one of the most widely used metals in industry, particularly where its properties of light weight and relatively high temperature resistance are required. Since material properties could be improved for alloys used in industry, research of this kind may have many practical applications. Typical problems of Al alloys include resistance to applied stress under high temperatures (creep), corrosion, fracture, and oxidation. Recent technological advances, including 3DAP, have made it possible for materials science research to progress from macro and micro scales down to the nano and subnanoscale levels. Today, researchers can view the compositional differences of the multicomponent alloys with an atomic-scale resolution.

The purpose of this research project was to investigate the precipitation strengthening of the Al(Sc) alloy through ternary addition of Ti. The composition of the alloy in question was Al 0.14wt% Sc 0.16wt% Ti. This ternary system was subjected to a detailed analysis, employing such methods as Vickers microhardness test, transmission electron microscope, and 3DAP. The objective was to verify that Ti migrates into the Al_3Sc $L1^2$ precipitate to form $Al_3(Sc_{1-x},Ti_x)$. If it does, it might cause changes to the lattice mismatch between the precipitate and the matrix, which, in turn, could decrease the coarsening rate and increase creep resistance of the intermetallic alloy.

Background

Although aluminum is fairly soft and exhibits little creep resistance, its microstructural and mechanical properties are drastically improved by adding other alloying elements such as scandium. Adding these elements strengthens the alloy's resistance to recrystallization, refines its grain structure during casting or welding, and enhances its superplastic properties.[1,2] The aeronautical industry has a great need for such alloy properties because Al is used in manufacturing blades and other components of jet engines.[2] While today's multicomponent alloy systems exhibit much better properties than those of even a few years ago, the need for materials with even greater strength and durability still drives many material science research laboratories across the globe. At Northwestern University, two recent studies focused on the dependence of mechanical properties and creep resistance of Al-based alloys containing Sc (Marquis and Fuller 2003).[5,6,8] These alloys form complex multicomponent systems that are difficult to study. Observations made during this research provide insight into the factors governing the evolution of the Al(Sc) precipitates, their growth at ambient and elevated temperatures, and effects that a ternary addition of elements such as Zr and Mg might have on the microstructure of these systems.

Approach

Alloy Casting, Homogenization, and Heat Treatment

One Al 0.14 at% Sc 0.16 at% Ti alloy was prepared by melting together two master alloys: Al-2.1wt% Sc and Al-4.68wt% Ti with 99.987wt% pure aluminum in air. The Al-Sc alloy was obtained from the Ashurst Corp., and the Al-Ti alloy was obtained from Alcoa Inc. Alcoa Research Laboratories' Analytical Chemistry Division verified the chemical composition of the Al-Ti master alloy. The Al was melted at 650˚C before the other two components were added. The

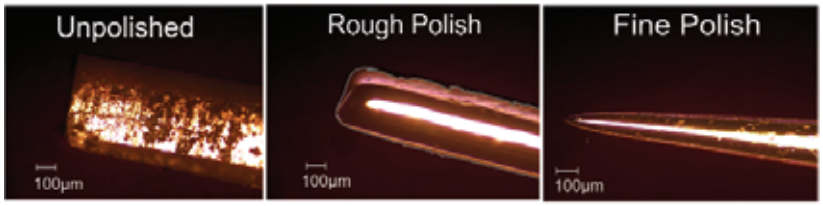

Figure 1: Three stages of the tip preparation for the 3DAP microscope. The radius of the apex of the tip in the last photograph is close to 50 nm.

melting was done in the alumina (Al_2O_3) crucible and stirred periodically with an alumina rod. Once all the solid components were liquefied, the melt was cast into a graphite mold and placed on a thick copper plate. Homogenization in the single-phase region of the ternary alloy was performed at 650°C for a period of 24 hours. Once homogenization was completed, the alloy was water quenched at ambient temperature and dissected using a slow-speed diamond saw into circular sections 1 cm in radius and about 0.5 cm thick. The disks then were annealed in a programmable air furnace within the two-phase region at 300°C for times varying from 15 minutes to 128 hours, followed by an immediate water quench to room temperature.

Vickers Microhardness Sample Preparation
All of the heat-treated samples were subjected to Vickers microhardness test. Prior to analysis, the disks' surface was polished down to a 1 micron level using different polishing wheels and various types of colloidal diamond suspensions. This ensured proper lubrication and avoided damaging and scratching of the samples. Vickers microhardness was measured using a 200 g load and an indentation time of 10 seconds. Fifteen independent measurements were performed for each of the samples analyzed. It is important to note that individual indentations were separated at least three radii apart to avoid possible alteration of data due to the presence of strain fields surrounding individual notches. The advantage of using Vickers microhardness techniques is that it gives a relatively quick and straightforward answer regarding sample hardness, which, in turn, makes it easy to determine if more advanced and time-consuming analysis of the sample at the nanoscale is required.

Transmission Electron Microscope
The transmission electron microscopy (TEM) sample was prepared by mechanically grinding a metal foil obtained from the sample and aged for 16 hours at 300°C to a thickness of about 220 µm. From such a prepared sample, disks averaging 2.5–3.0 mm in diameter were mechanically ground out and twin-jet electropolished with a Struers Tenupol, using solution of 5 vol% perchloric acid in methanol at -30°C and 13.6V, until perforation. The sample was then analyzed for precipitate radii, crystal structure, and possible defects on a Hitachi 8100 transmission electron microscope operating at 200kV.

Three-Dimensional Atom Probe
3DAP analysis, which is a combination of a field ion microscope (FIM) and a mass spectrometer of single-ion sensitivity,[2] requires very careful tip preparation using a two-stage electropolishing sequence. In this study, the first step of tip preparation was obtaining a needle-like sample from a larger portion of the alloy approximately 700 µm x 700 µm thick. The second step involved pulse-electropolishing the cut sample using electrolyte of 10% perchloric acid in acetic acid. Finally, the electrolyte was changed to 2% perchloric acid in butoxy, thus guaranteeing a precise cleaving of the material of the prepared tip (Figure 1).

It is important to note that tip preparation is crucial for successful 3DAP analysis. The diameter of the apex of the tip has to be less than 100 nm (preferably <50 nm) to guarantee its proper development and a bright, crisp image of a relatively high resolution. If the radius of the tip is too large, the electric field at the tip will be too low, and it will be impossible to evaporate atoms. 3DAP also allows atom-by-atom dissection of a small volume of a material, resulting in in-depth, three-dimensional analysis. Before such analysis was obtained, an FIM image was acquired after one hour of tip development. The imaging gases were He and Ne, respectively. The primary detector was placed near the [111] pole for the proper crystallographic orientation for 3DAP analysis. Field evaporation was performed at 30K with a pulse fraction of 20%.

MacOS-based application software: ADAM 1.5b13
The final step of the three-dimensional data analysis relied on "ADAM," a MacOS-based application that was developed and modified by members of Seidman's group. This software analyzes the data collected from the FIM and 3DAP microscopy by performing a set of

calculations that give a three-dimensional reconstruction and visualization of the arrangement of the atoms, concentration maps, concentration profiles, proxigrams, concentration distribution, and isosurfaces.[3,4] Without this analytical software, data analysis for the 3DAP and entire three-dimensional reconstruction would be very challenging.

Results and Discussion

Microhardness

Table 1 represents a set of microhardness values obtained for the Al-0.14wt% Sc 0.16wt% Ti aged at different times. The graph of a microhardness versus aging time curves for four different alloys — three of which are binary Al(Sc)5 and one ternary Al(Sc, Ti) — is given in Figure 2. All of these curves represent the changes in Vickers microhardness after aging at 300°C for various times and demonstrate the four regions of precipitation-strengthened alloys: incubation of decreasing duration with increasing temperature; rapid increase in hardness (underaging); a plateau at the highest hardness values (peak aging); and decrease in hardness values with increasing aging time (overaging).[5,6]

Although both Al-0.3 wt% Sc and Al-0.14 wt% Sc 0.16 wt% Ti alloys have an equal volume fraction of precipitates, Al-0.3 wt% Sc alloy reaches much higher hardness values. Therefore, it is valid to say that the Sc contribution to alloy hardening is much greater than that of Ti. Also important to note is the fact that the binary Al-0.3 wt% Sc alloy reached peak hardness values much earlier than the ternary Al-0.14 wt% Sc 0.16 wt% Ti alloy. This indicates that the coarsening for binary alloy will occur faster (greater kinetics) than for the ternary system.

Minutes	0.0	15.0	30.0	60.0	120.0	480.0	960.0	1920.0	7680.0
Seconds	1	900	1800	3600	7200	28800	57600	115200	460800
Microhardness									
1)	22.6	22.4	21.0	21.6	24.6	31.9	41.5	41.5	40.2
2)	20.7	2.0	22.1	21.5	24.4	34.1	46.5	41.2	39.8
3)	21.3	22.9	21.7	21.0	24.0	32.1	42.2	41.0	41.8
4)	22.7	22.4	21.7	21.6	22.6	34.2	43.0	42.3	44.1
5)	20.7	23.1	21.1	21.4	22.6	34.7	40.1	44.6	42.3
6)	20.7	22.4	21.2	20.2	22.3	30.9	41.0	39.3	39.2
7)	20.1	20.2	21.2	22.6	22.4	34.9	43.3	42.2	44.9
8)	20.4	21.3	22.0	21.8	23.0	33.3	41.5	42.3	40.8
9)	19.0	21.6	22.4	19.4	21.2	31.3	42.4	43.2	45.4
10)	20.9	22.6	20.0	21.5	23.7	31.6	42.2	44.6	47.9
11)	20.6	20.3	22.4	22.5	22.6	33.6	40.6	45.3	43.3
12)	19.7	21.8	21.0	21.5	22.9	34.7	40.2	47.0	38.0
13)	20.3	21.9	20.9	21.9	22.7	34.2	41.0	40.9	42.3
14)	19.5	22.8	21.4	22.2	22.3	34.7	40.9	44.9	42.2
15)	19.3	23.0	21.5	21.4	22.9	34.4	40.6	44.1	41.1
Average Microhardness	20.6	20.6	21.4	21.5	22.9	33.4	43.0	43.0	42.2
MPa	**201.6**	**201.6**	**210.1**	**210.4**	**224.8**	**327.1**	**420.9**	**420.9**	**413.8**
Standard Deviation	1.0574	5.050837	0.638972	0.815621	0.895066	1.413439	1.627004	2.072565	2.599231
	10.36252	49.4982	6.261929	7.993099	8.771645	13.8517	15.94464	20.31113	25.47246

Table 1: Microhardness values for nine samples of the Al(Sc,Ti) alloy aged at various times starting from 15 minutes up to 128 hours. The peak microhardness was reached after 16 hours and was equal to 420.9MPa.

Furthermore, the microhardness values for the ternary alloy demonstrate that the addition of 0.16 wt% Ti to the binary system of Al 0.14 at% Sc did not introduce a significant precipitation hardening effect in comparison with the binary system of Al 0.1 at% Sc. Because there is little data for the Al 0.14% Sc binary system, it is difficult to compare these two systems, yet an indirect evaluation of both of the data curves is perfectly legitimate. The increased hardness values of the ternary alloy can be attributed to the presence of a significant amount of Sc (0.14wt%). Therefore, it is questionable whether the Ti present (0.14wt%) has any effect on strengthening of the alloy.

Transmission Electron Microscope

TEM analysis of the sample alloy heat-treated at 300°C for 16 hours revealed some interesting facts. Visible in the bright-field image at magnification of 100,000x are nanoscale-size, coherent, and spherical precipitates of $Al_3(Sc_{1-x},Ti_x)$ (Figure 3c). Their high volume fraction and number density signifies their contribution to the increased hardness of the Al(Sc, Ti) alloy. Also important is the fact that those precipitates were homogeneously distributed throughout the two-phase ternary alloy system, providing additional evidence for their coherency. This information is crucial to studying and understanding the mechanism that leads to the growth and coarsening phases that occur during decomposition of the alloy when it is subjected to high temperatures for an extended period of time. It is desirable to have the highest number of small and coherent precipitates evenly dispersed throughout the matrix so that they can act as obstacles for the dislocation movement. The more difficult the movement of these dislocations, the slower the coarsening rate; the higher the

high-temperature resistance, the higher the creep resistance of the alloy. The TEM analysis is important, but it does not provide precipitate composition profiles. Thus, further 3DAP analysis of the sample is required. Figures 3a and 3b represent the image of a diffraction pattern aligned along the [011] crystallographic pole of the investigated alloy. The black spots represent the electron beams being diffracted from the Al3(Sc1-x,Tix) precipitates. The intersecting Kikuchi lines are also present, and their cross-section shows the localization in [110] direction.

Field Ion Microscope and 3DAP Data Analysis

The FIM image was obtained before the 3DAP data was collected. Figure 4 represents the actual FIM image resolved during field ionization of the imaging gas particles interacting with the atoms located at the apex of the specimen. This interaction represents electrons tunneling from the field-absorbed gas atoms into the metal, and finally repulsion of the positively charged gas ions toward the phosphor screen.[7] The brightly imaged spots are actually the individual solute atoms (Sc or Ti), while the surrounding irregular dark areas are the aluminum matrix. While acquiring this image, the primary detector was located near the [111] crystallographic pole, illuminating the atomic planes perpendicular to the direction of field-evaporated ions/ direction of analysis. The most interesting part of this image is the presence of the lines of decoration, which are representative of local variation in the tip radius (difference in the electric fields) and other material parameters.[7]

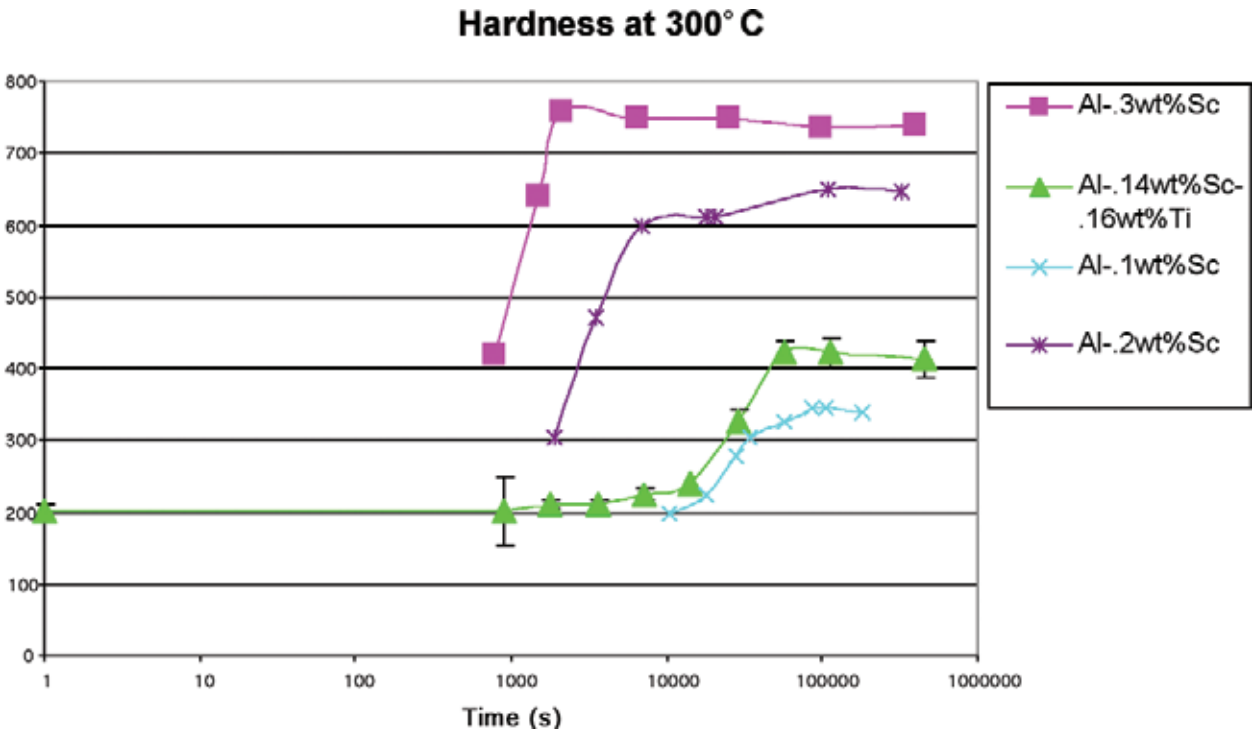

Figure 2: The graph of the hardness values (MPa) versus the aging time of the of the Al-0.14wt% Sc 0.16wt% Ti, in comparison to the other binary Al(Sc) alloy systems. It is not clear if the increase in the hardness values of the ternary alloy resulted due to presence of Ti or additional amounts of Sc in comparison with the Al-0.1 wt% Sc binary alloy system.

Figure 5 represents three-dimensional reconstruction of the Al matrix showing densely packed atomic {111} planes, with the interplanar spacing d111=0.236 nm. Since the tip subjected to analysis was of a hemispherical shape and the field-evaporated ions were projected onto a two-dimensional position-sensitive detector, the reconstructed planes exhibit a peculiar curvature.[8]

Time-of-flight mass spectra represented by three consecutive histograms (Figure 6) are indicative of the atomic species/elements present in the alloy according to their mass-to-charge ratios. All of the elements, including Al, Ti, and Sc, have their representative peaks at appropriate values. In addition, there are several very pronounced peaks present for the metal hydrides of (AlH)+, (AlH_2)+, and (AlH_4)+, as well as for the (ScH)+ and (ScH_2)+. This detailed analysis helped in estimating various ratios of imaged ions and provided additional information regarding possible presence of impurities in the analyzed sample.

A proposed model of the actual isoconcentration surface is presented in Figure 7, where the red atoms represent the $L1_2$ alloy-strengthening phase, and the surrounding purple area is the aluminum matrix with small amounts of Sc and Ti atoms evenly distributed throughout. The proximity histogram (proxigram) was used to determine the composition of the precipitate phase based on the atomic fraction of the alloying elements. The proxigram is a plot of concentration versus distance and is analogous to a linear concentration profile, where the value of zero is representative of the position of the actual á-Al/Al_3Sc interface of the precipitate (outermost boundary of the isoconcentration surface) separating it from the

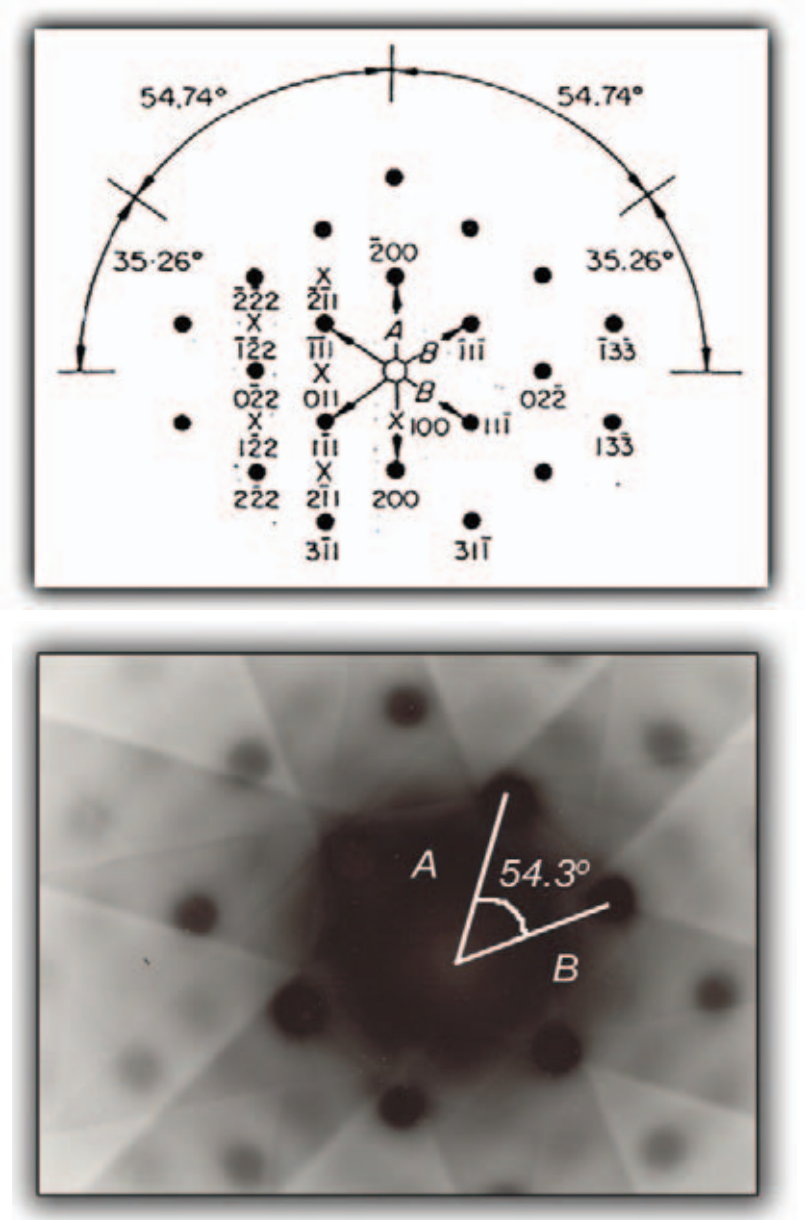

Figures 3a, 3b: Diffraction pattern aligned along the [011] crystallographic pole of the investigated alloy. Visible are the beams of electrons diffracted from the $Al_3(Sc_{1-x},Ti_x)$ precipitates, as well as the Kukuchi lines.

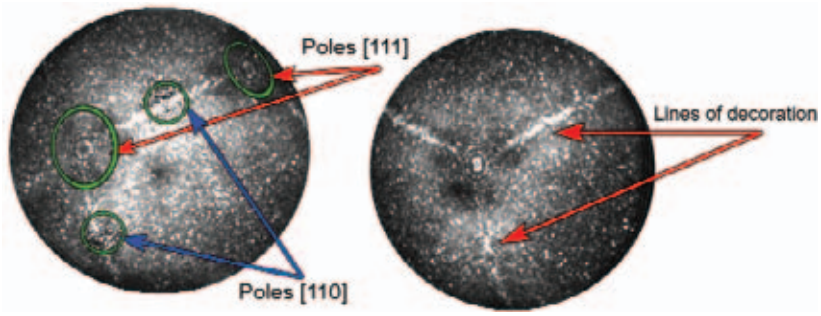

Figure 4: The FIM images of the Al-0.14wt% Sc 0.16wt% Ti alloy aged at 300°C for a period of 16 hours. In the first image, the blue arrows point toward the [110] poles, while the red arrows point toward the [111] crystallographic poles. Lines of decoration, which are known to be the result of a variation in the tip radius and other material parameters, are present in the second image.

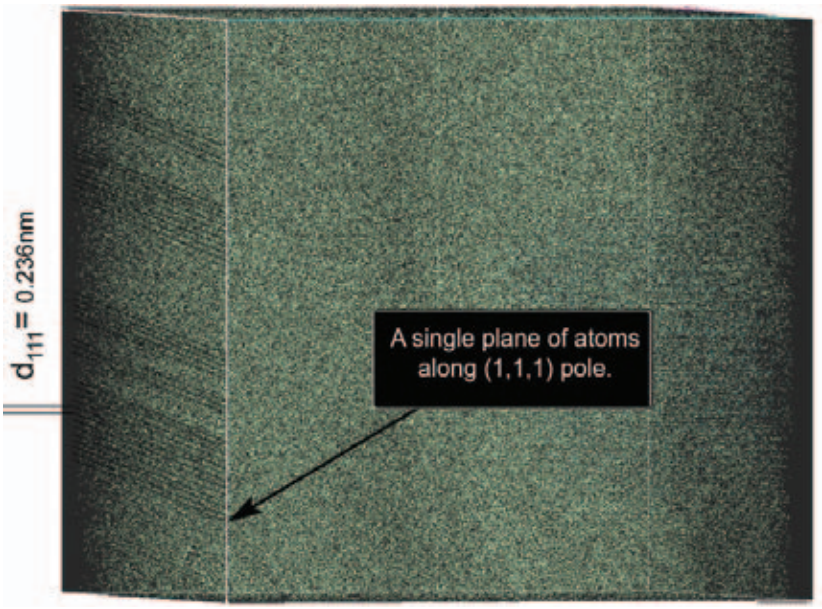

Figure 5: Three-dimensional reconstruction of the Al(Sc,Ti) matrix. Visible presence of the planes of atoms, with the intermediate interplanar spacing d_{111}=0.236 nm.

rest of the matrix.[9] The positive values indicate decreasing radii (here, moving away from the interface toward the center of the precipitate). The negative distance values, on the other hand, correspond to the points (atoms) located on the outside of the precipitate in the matrix (here, away from the isoconcentration surface). On the proxigram obtained for Al-0.14wt.%Sc 0.16wt%Ti, presented as Figure 8, it is clearly visible that both of the alloying elements, Sc and Ti, did segregate into the precipitate and/or formed the previously expected $Al_3(Sc_{1-x},Ti_x)$ $L1_2$ phase. The fact that Ti actually substituted into the Al_3Sc precipitate, and possibly replaced some of the Sc, is of crucial importance to the outcome of this research. Ti simply substituting into the $L1_2$ phase can decrease the lattice mismatch between the aluminum matrix and the precipitate.

The lattice parameter of pure aluminum and precipitate phase of Al3Sc is equal to 4.095 nm and 4.100 nm, respectively.[9] Although the difference in the lattice parameter is small, its further decrease is suspected to have a positive effect on the microstructural properties of the alloy. Smaller lattice mismatch increases the size at which the precipitates become semicoherent. Because semicoherent precipitates coarsen much faster, this effectively reduces the coarsening rate (when an alloy coarsens there will be fewer precipitates to act as a barrier to dislocations). Also, because the creep resistance is directly correlated to the coarsening rate, decreasing the coarsening rate automatically increases alloy's creep resistance.

Conclusions

The Al-0.14 wt% Sc 0.16wt% Ti reached its peak hardening after 16 hours of heat treatment at 300°C. The supersaturated solid-solution decomposed into the Al matrix and numerous nanoscale L12 phase precipitates of $Al_3(Sc_{1-x},Ti_x)$. Titanium — possibly by partitioning and/or substituting into the Al3(Sc) — might have decreased the lattice mismatch between the Al matrix and the precipitate and decreased the coarsening rate, which subsequently increased its creep resistance properties. Although such substitution occurred, the microhardness values of the ternary alloy did not increase drastically compared with the Al-0.1wt% Sc binary two-phase alloy system. These results are important, but the research is far from complete. It is imperative to analyze more samples of the same alloy at different aging times and temperatures to compare microstructural evolution of their precipitates, their special distribution, number densities, and other crucial properties. This analysis may provide further insight into the principles that govern the process of decomposition and early-stage transformation of these complex multicomponent systems.

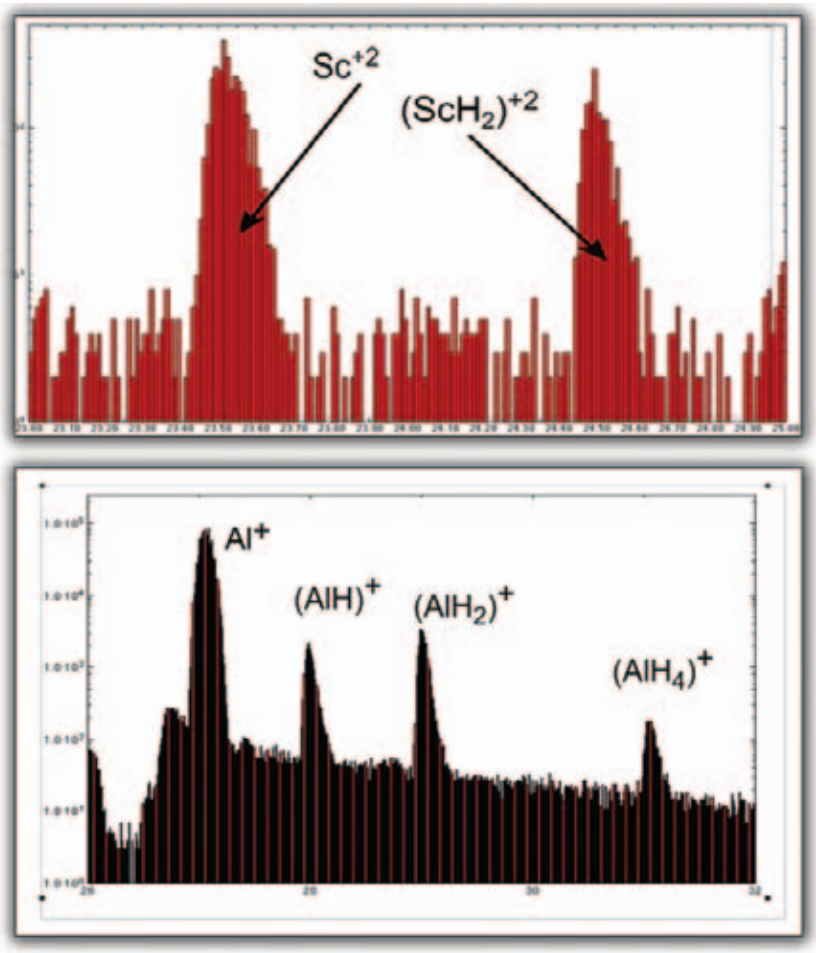

Figure 6: Histogram of number of detected ions vs. their mass-to-charge ratios. Present are the peaks for Al and Sc ions as well as their hydride forms.

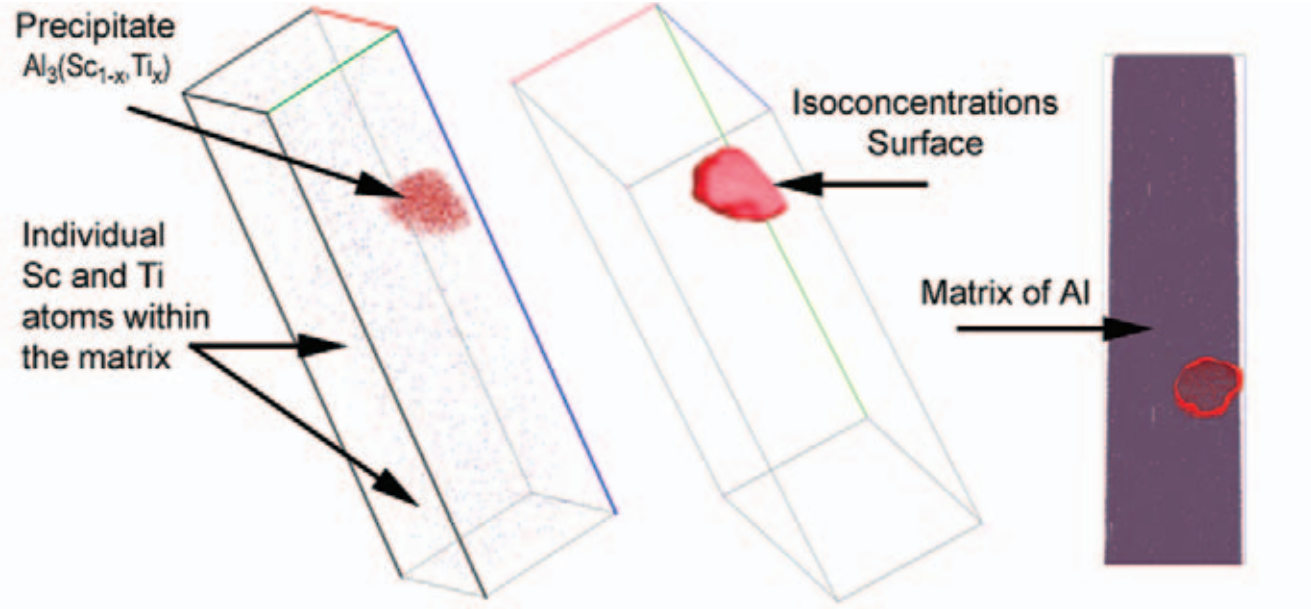

Figure 7: Three-dimensional reconstruction of an analyzed volume from the Al-0.14wt% Sc 0.16wt% Ti alloy aged at 300°C for a period of 16 hours. Individual atoms of Al-purple, Ti-blue, and Sc-red. Clearly visible increased density of the Sc and less of the Ti atoms at the site of the precipitate (inside of the Al/Al_3Sc interface).

References

(1) Toropova, L. S.; Eskin, D. G.; Kharacterova, M. L., et al. *Advanced Aluminum Alloys Containing Scandium;* Overseas Publishers Association: Amsterdam, 1998.

(2) Scandium in Aluminum Alloys. http://www.home.no/al-sc/index.html August 2003.

(3) Hellman, O. C., et al. *Mater. Sci. Eng. C* **2001**, *513*, 29.

(4) WebElements, the Periodic Table on the WWW: Aluminum. http://www.webelements.com/webelements/elements/text/Al/xtal.html August 2003.

(5) Marquis, E. A.; Seidman, D. N.; Dunand, D. C.; *Acta Mater.* **2003**, in press.

(6) Fuller, C. B.; Seidman, D. N.; Dunand, D. C. *Acta Mater.* **2003**, *51*, 4803.

(7) Miller, M. K.; Smith, G. D. W. *Atom Probe Microanalysis*; Material Research Society: Pittsburg, PA, 1989, p 3.

(8) Marquis, E. A.; Seidman, D. N.; Asta, M., et al. *Phys. Rev. Lett.* **2003**, *91*, 036101.

(9) The Seidman Research Group. http://grain.ms.northwestern.edu/tools/adam/adam.html August 2003.

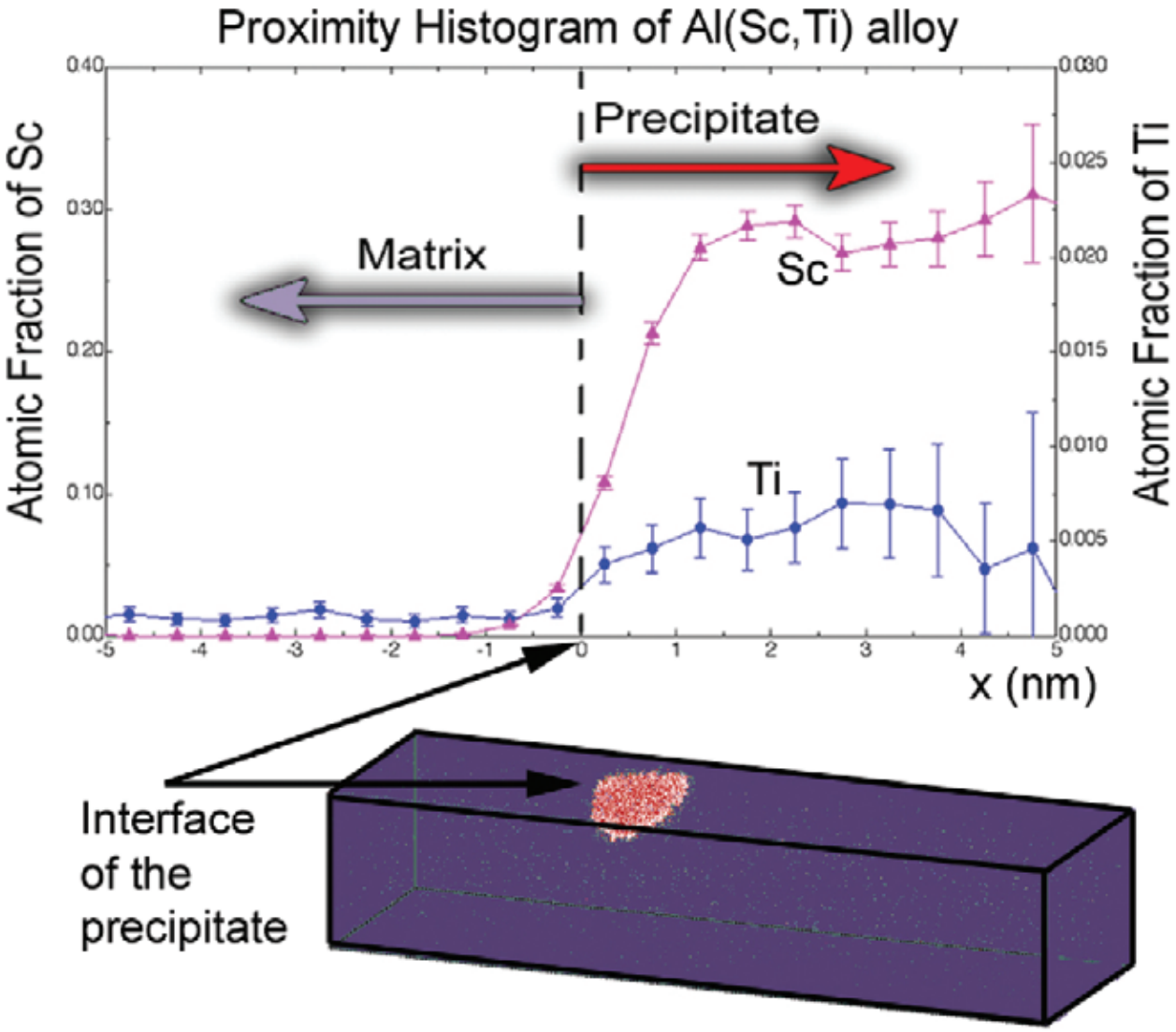

Figure 8. Proximity histogram representing atomic fraction of each of the alloying element (Sc and Ti). Shown are the concentrations of Sc and Ti with respect to distance from the α-Al/Al_3Sc interface. Visualization and graphical representation performed using the ADAM 1.5b13 software.